DOT/FAA/PM-87-37

Project Report
ATC-155

Storm Models for End-to-End TDWR Signal Processing Simulation Tests

J. E. Evans

1 May 1989

Lincoln Laboratory
MASSACHUSETTS INSTITUTE OF TECHNOLOGY
LEXINGTON, MASSACHUSETTS

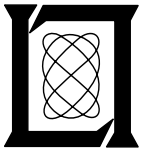

Prepared for the Federal Aviation Administration,
Washington, D.C. 20591

TECHNICAL REPORT STANDARD TITLE PAGE

1. Report No.	2. Government Accession No.	3. Recipient's Catalog No.
DOT/FAA/PM-87-37		

4. Title and Subtitle	5. Report Date
Storm Models for End-to-End TDWR Signal Processing Simulation Tests	1 May 1989
	6. Performing Organization Code

7. Author(s)	8. Performing Organization Report No.
James E. Evans	ATC-155

9. Performing Organization Name and Address	10. Work Unit No. (TRAIS)
Lincoln Laboratory, MIT P.O. Box 73 Lexington, MA 02173-0073	11. Contract or Grant No. DTFA-01L-83-4-10579
	13. Type of Report and Period Covered
12. Sponsoring Agency Name and Address Department of Transportation Federal Aviation Administration 800 Independence Avenue, SW Washington, DC 20591	Project Report
	14. Sponsoring Agency Code

15. Supplementary Notes

The work reported in this document was performed at Lincoln Laboratory, a center for research operated by Massachusetts Institute of Technology under Air Force Contract F19628-85-C-0002.

16. Abstract

End-to-end qualification testing of the Terminal Doppler Weather Radar (TDWR) contractor signal processing system will be accomplished by a signal processing simulation test. Government furnished storm models will be used to provide inputs to the signal processor. The corresponding hazardous weather product results will be compared to the results determined by the detection algorithm developers. This report examines the role of the end-to-end tests in the context of overall TDWR qualification testing and concludes that the signal waveform/velocity ambiguity resolution should be the principal focus of the signal processing simulation testing. Salient characteristics of the initial pair of storm models (a high reflectivity microburst observed in Huntsville, AL, and a series of low-to-moderate reflectivity microburst storms observed in Denver, CO) are described as well as desirable characteristics of additional storm models to be provided later.

17. Key Words		18. Distribution Statement
Terminal Doppler Weather Radar microburst	algorithm waveform/velocity signal processing	Document is available to the public through the National Technical Information Service, Springfield, VA 22161.

19. Security Classif. (of this report)	20. Security Classif. (of this page)	21. No. of Pages	22. Price
Unclassified	Unclassified	72	

FORM DOT F 1700.7 (8-69)

ABSTRACT

End-to-end qualification testing of the Terminal Doppler Weather Radar (TDWR) contractor signal processing system will be accomplished by a signal processing simulation test. Government furnished storm models will be used to provide inputs to the signal processor. The corresponding hazardous weather product results will be compared to the results determined by the detection algorithm developers. This report examines the role of the end-to-end tests in the context of overall TDWR qualification testing and concludes that the signal waveform/velocity ambiguity resolution should be the principal focus of the signal processing simulation testing. Salient characteristics of the initial pair of storm models (a high reflectivity microburst observed in Huntsville, AL, and a series of low-to-moderate reflectivity microburst storms observed in Denver, CO) are described as well as desirable characteristics of additional storm models to be provided later.

TABLE OF CONTENTS

LIST OF ILLUSTRATIONS

LIST OF TABLES

I. INTRODUCTION

The Terminal Doppler Weather Radar (TDWR) system is designed to provide real time information on hazardous terminal area weather (especially wind shear) to Federal Aviation Administration (FAA) Air Traffic Control (ATC) personnel and, eventually, via the Mode-S data link, to pilots. Full end-to-end testing of a TDWR contractor system to validate all the key contractor provided system features for system acceptance is complicated by the practical difficulty in arranging for appropriate "test" storms and "truth" data at the contractor test site. Consequently, a multifaceted test program has been developed for the TDWR contractor system validation.

This report describes one element of the validation program: a set of storm models based on actual measured storm data from appropriate meteorological regions. They will be used for end-to-end simulations that evaluate the contractor-designed signal waveforms and weather parameter estimation algorithms as well as the contractor implementation of the weather detection algorithms.

In this introduction, we highlight the principal technical features and issues which arise in testing a TDWR. Chapter II describes how various elements of the TDWR will be tested and the role of the end-to-end simulation tests in the overall process. Chapter III describes the initial set of weather models to be used for the end-to-end testing. Chapter IV summarizes the results and discusses the desired features of other end-to-end test cases which will be provided subsequently.

Figure I-1 shows a high level functional block diagram of the TDWR. The Radar Data Acquisition (RDA) section is responsible for acquisition and signal processing of base data, clutter suppression, control, monitoring, and base data error detection. The RDA hardware consists of the antenna/mount, the transmitter, receiver, and signal processing equipment.

The Radar Product Generation (RPG) section is responsible for control command generation and real time product generation. The government provided algorithms for wind shear detection will be coded (in a high order programming language) by the TDWR contractor to operate on the contractor general purpose computer. The RPG also provides for the real time control of the TDWR operating mode, signal waveform (i. e., PRF) as well as product archiving.

The initial TDWR display function consists of controller's alphanumeric (ribbon) and supervisor's situation displays and will be superseded by other displays, not part of the TDWR project, in the end-state National Airspace System (NAS). The ribbon display will be an alphanumeric display with audible and visual alarms for use at the Air Traffic Control Tower (ATCT) and the Terminal Radar Approach Control facility (TRACON) which presents hazardous warnings that are to be read verbatim to pilots affected. The situation display will supply area wide weather information which will be used to assist the ATCT and TRACON supervisors in making strategic decisions as to airport configuration and traffic flow.

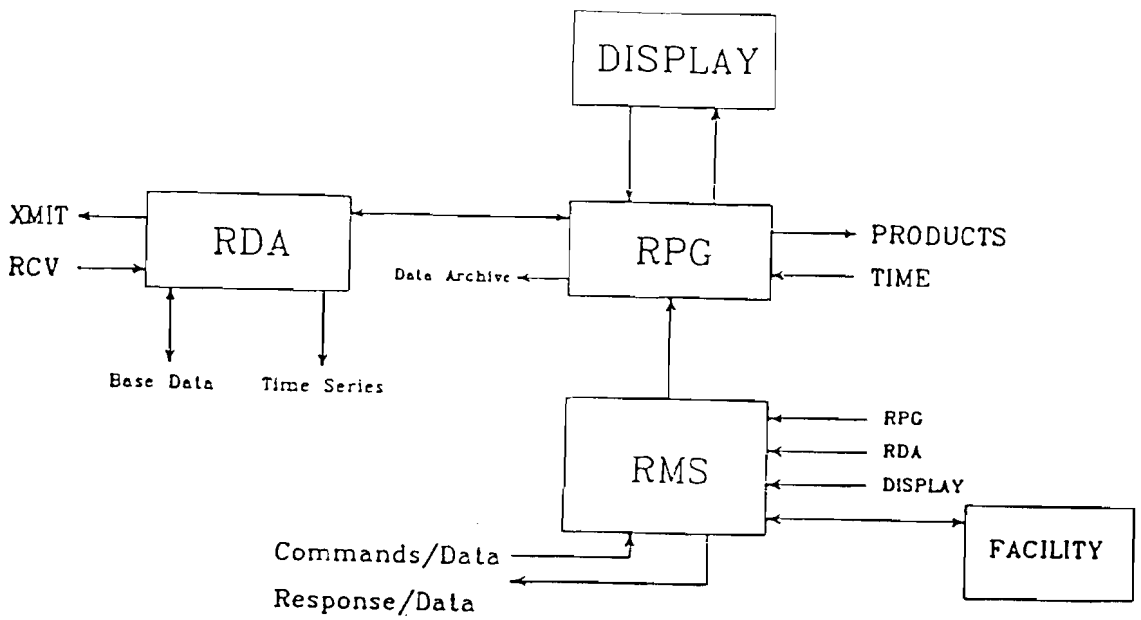

Figure I-1. System Functional Relationships. TDWR monitoring via the Remote Maintenance System (RMS) is not addressed in this report because it serves primarily to insure that the TDWR is operating as designed.

Table I-1 shows the respective responsibilities of the government and contractor for the principal system elements which are associated with weather detection by a TDWR*. The allocation of the various responsibilities is an important factor in the overall testing process for the TDWR contractor since it is neither feasible nor appropriate for contractor tests to verify all of the government specified features.

In particular, key system drivers such as wind shear event characteristics (e. g. reflectivity levels, physical size as a function of time, velocity signatures, etc.) and environmental factors (e. g. clutter levels, rain attenuation, out-of-trip weather characteristics) have been determined by a series of scientific and operationally oriented measurements and numerical modeling over the past decade. A comprehensive testing program to readdress all of the drivers and the associated government-specified features using the TDWR contractor first production system would take many years and likely provide only a marginal improvement over the current estimates of the weather and environmental characteristics.

Similarly, the government-furnished algorithms have been developed on the basis of a number of years of measurements and testing with appropriate supporting weather measurement sensors. Further testing and refinement of the algorithms will occur prior to the TDWR contractor first unit delivery. To fully test and verify in detail the TDWR government supplied algorithms would require a time period comparable to that used for the algorithm development.

In view of the above considerations, we conclude that the TDWR contractor system testing should focus on determining that contractor-specified system elements will both meet its explicit requirements (e.g., antenna beamwidth dynamic range, throughput, and response times) and enable the TDWR to meet its overall goals.

Chapter II describes how the bulk of the contractor specified features shown in Table I-1 are to be tested. Many of these "standard" radar testing issues (e. g., antenna pattern characterization, power budget verification, mount capability assessment, receiver dynamic range confirmation) are straightforward. Others (e. g., weather parameter estimation method validation and certain aspects of clutter suppression performance) are unique to weather radar applications, but also well understood and relatively easy to test. In Chapter II, we discuss how certain key tests may be accomplished.

* The TDWR monitoring via the Remote Maintenance System (RMS) and reliability features are not shown in Table I-1, nor addressed in this report on the grounds that they serve primarily to insure that the TDWR is operating as designed.

Table I-1
TDWR System Responsibilities for Key Elements of TDWR
Weather Detection Performance

SPECIFIED BY	RDA	RPG	DISPLAY
Government	antenna beamwidth scanning patterns dynamic range weather signal and parameter accuracy ground clutter suppression range obscuration avoidance	hazardous weather detection algorithms throughput product formats	display characteristics, throughput and response times product formats
contractor	transmitter characteristics signal waveforms rf components. receiver type and features weather parameter estimation methods velocity ambiguity resolution bad data flagging signal processing implementation	algorithm implementation (computer and software architecture) product communications	display systems product communication

The greatest challenge in TDWR qualification testing is dealing with contractor-dependent data quality features and all of the sources of error in weather parameter measurements. Although there are many key system features which are contractor-specified, many of these (e. g., transmitter power and receiver linearity) are very heavily constrained by the overall TDWR requirements (e. g., minimum detectable signal, scan strategy, and clutter suppression). The principal area for contractor differences which may substantially impact weather detection performance is waveform design and range velocity ambiguity resolution. Different choices of signal waveform (i. e., pulse spacing) can yield dramatic differences in the range/velocity ambiguity resolution logic (Doviak and Zrnic', 1984, Zrnic', 1985) and accuracy of the resulting velocity estimates. The performance of the major wind shear detection algorithms can be significantly affected by the quality of the velocity estimates. Consequently, Chapter III focuses on weather models which consider situations where difficulties may arise in achieving the required quality of velocity data.

The other major area of difficulty that arises is modeling all the sources of error in the weather parameter measurements. Classically, radar meteorology system designers have been concerned with weather signal-to-noise effects and weather process statistical fluctuations (see e. g., Doviak and Zrnic', 1984). However, practice has shown that measurements in the surface boundary layer with TDWR-like radars encounter a plethora of other error sources which are poorly understood in a statistical modeling sense. They include

(1) clutter from moving scatters such as planes, birds, and vehicles which is not attenuated by the TDWR high pass clutter filters (or functional equivalent);

(2) the residual clutter from strong stationary clutter sources;

(3) very small spatial scale variations in the velocity field within a beam volume (e. g., due to localized shadowing or meteorological phenomena such as "dust devils").

Experience has shown that the additional error sources cited above are very important factors in the algorithm design. In particular, the use of idealized wind fields (e. g., as produced by a radially symmetrical model microburst) with only the "classic" error sources are likely to give much more optimistic results than can be achieved in practice. Lacking a carefully validated model for these additional "nonclassical" error phenomena, the recommended alternative is to use actual measured data sets to furnish realistic "fine grain" measurement errors while relying on expert human judgment to correct gross errors in the measured data sets. Actual measured data sets are used in the TDWR validation in two areas:

(1) testing the "correctness" of algorithm implementation (as discussed in Chapter II), and

(2) the end-to-end testing discussed in Chapter III.

Since it is important that the data sets have a representative component of "nonclassical" weather parameter errors, data from the FAA TDWR test-bed radar (Evans and Johnson, 1984) has been used exclusively since the other Doppler weather radars (e. g., those of the National Center for Atmospheric Research (NCAR) and the National Severe Storms Laboratory (NSSL)) did not use clutter suppression filters in their scientific wind shear studies. In Chapter III, we discuss the applicability of the TDWR test-bed data at S-band for end-to-end testing of the C-band TDWR.

II. TDWR SYSTEMS TESTING

A. FUNCTIONAL UNIT AND SUBUNIT TESTING

Much of the TDWR subunit qualification testing consists of examinations employed in ordinary radar practice: (1) antenna pattern measurement on a test range; (2) mount scanning capability verification using stop watches and conventional servo outputs; (3) transmitted pulse characterization using rf signal analyzers; and (4) power budget validation using transmitter, pulse, and receiver sensitivity measurements. Those tests do not need explanation and ennumeration here.

This report will instead focus on the several key tests which are either unusual or unique to the TDWR system or which have proven a difficulty in other procurements. This report will provide salient examples only. This report is not a complete dissertation on the topics discussed.

Figure II-1 shows the principal inputs and outputs used for TDWR functional testing of units and subunits.

1. Clutter Suppression Capability

Achieving high levels of clutter suppression in operational pulse Doppler radars requires careful attention both to the rf and to the digital processing subsystems. Accordingly the TDWR test program verifies both the key subsystems and the operation in qualification testing.

Figure II-2 shows the equivalent weather reflectivity as a function of range for various distributed clutter scattering cross section densities (σ_0). An urban environment illuminated near zero degrees might typically have a (σ_0) of -40 dB wrt $1m^2/m^2$, which would in turn necessitate approximately 50 dB clutter suppression to have an adequate signal to clutter ratio (e. g., +10 dB) for a dry microburst outflow (reflectivity +5 dBz).

The rf system is addressed by requiring direct measurements of the instability residue (See Paragraph 4.2.1.7.2 in FAA-E-2806.) using, for example, the time series port data or the TDWR processors to obtain the requisite spectra of the digitized time series data. Adequacy of the digital processing subsystem is demonstrated by the use of synthetic time series data using clutter models for distributed and discrete scatterers (Paragraphs 4.2.1.7.1 and 6.2.21 in FAA-E-2806).

Finally end-to-end clutter suppression is tested by demonstrating clutter suppression as the antenna scans a fixed, discrete clutter target (a radio tower, for example) as discussed in Paragraph 4.2.1.7.3 of FAA-E-2806.

2. Doppler Velocity Estimation

Verification of proper Doppler velocity estimation is very important in the TDWR. The moving target simulator (MTS) retransmits a received pulse at an offset frequency (Paragraph 3.1.4.1.6 of FAA-E-2806). Verification that the measured Doppler shift at the range gate corresponds to the expected Doppler shift provides an end-to-end test of the system IF control and signal processing computations. However, the MTS probes performance only at a given equivalent reflectivity and Doppler shift.

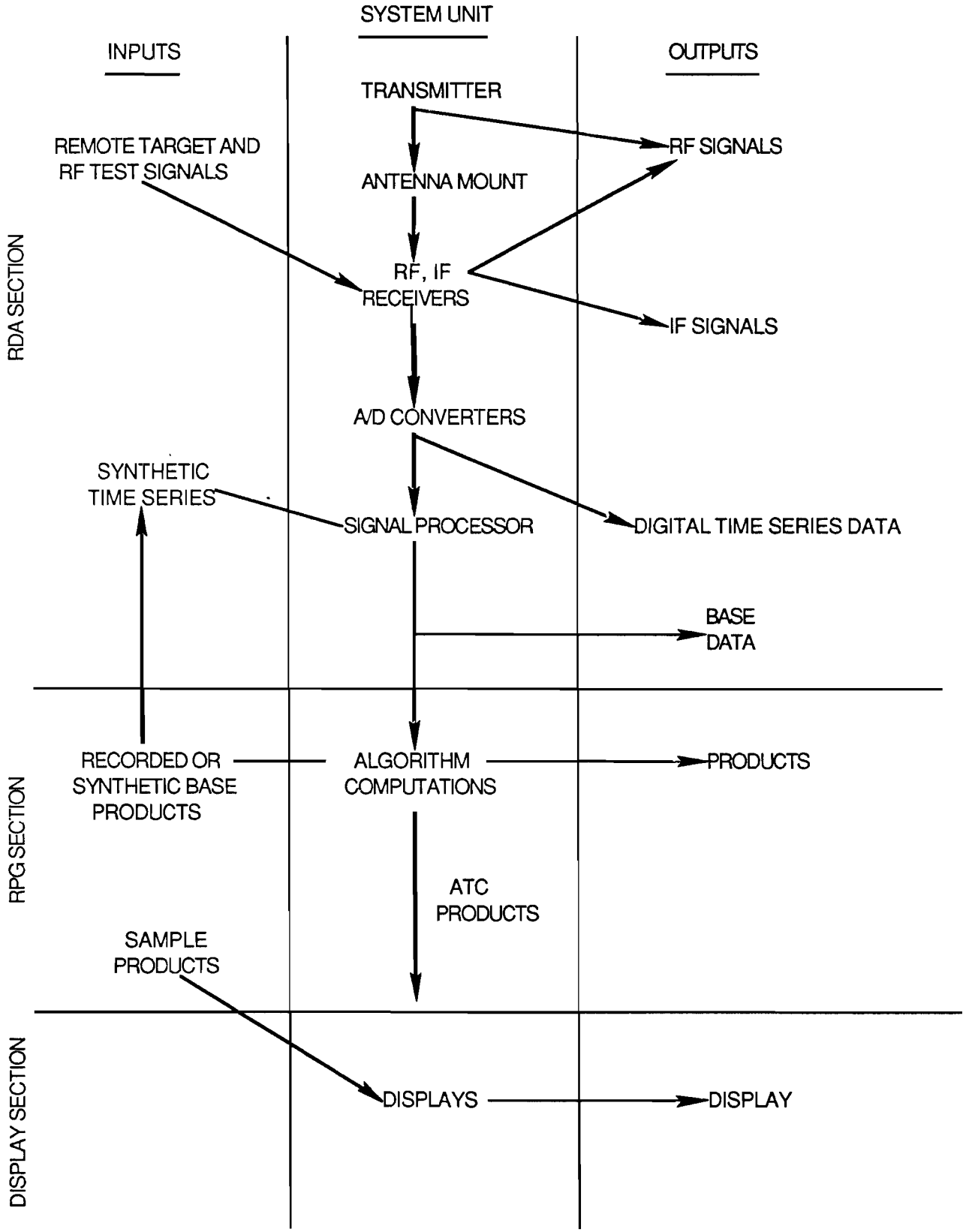

Figure II-1. Inputs and outputs for TDWR qualification testing.

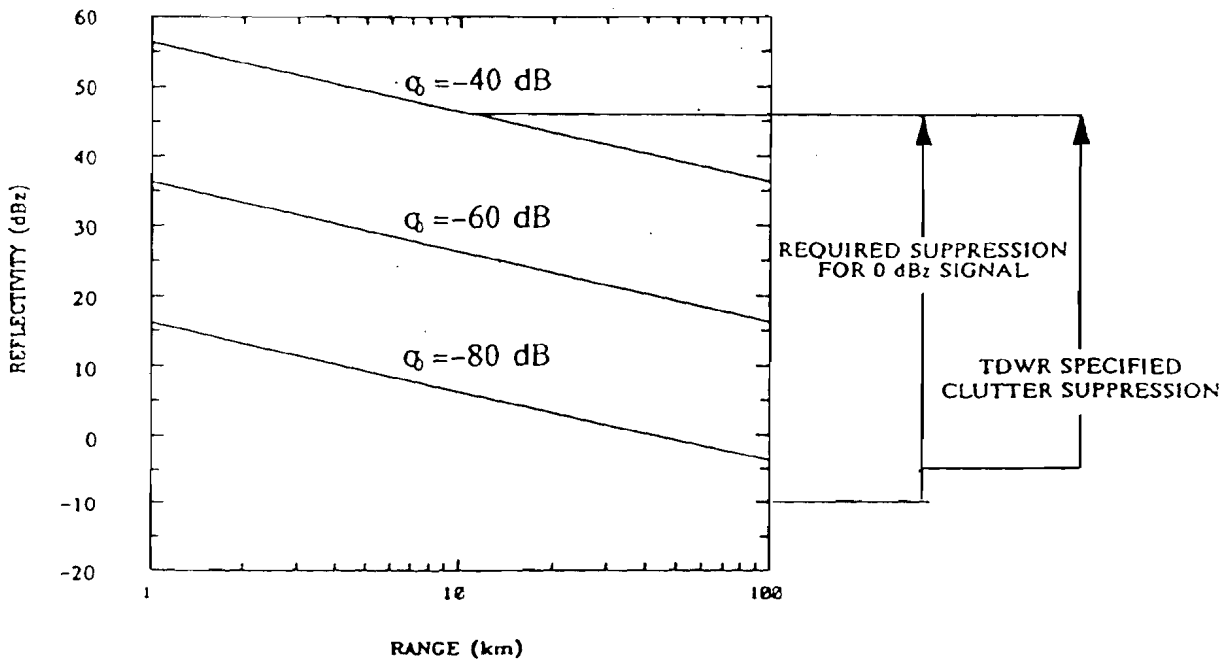

Figure II-2. Equivalent weather reflectivity for distributed clutter reflectivity levels.

3. Wind Shear Detection Algorithm Implementation

The algorithms which provide automated detection of wind shear hazards such as microbursts and gust fronts are being provided to the contractors in a generic description language (Merritt and Campbell, 1987, Sanford, Witt, and Smith, 1987) Thus, it is necessary to verify that the contractor has correctly implemented the algorithms in the language/computers used for the RPG.

In addition to the customary software development verification procedures, the government will supply the contractor with (1) base product data sets measured at various locations using the TDWR test-bed radar, and (2) algorithm outputs (e. g., wind shear locations and strengths) and intermediate results (e. g., shear feature fields) as computed by the algorithm developers.

By comparing the contractor results with the algorithm developer results for the same input sets, it will be possible to verify that the contractor implementation of the algorithms gives the same results as the field measurement verified software (paragraphs 4.2.1.10 and 4.2.1.11 in the FAA-E-2806).

B. ROLE OF END-TO-END SIMULATION TESTING

The various functional unit and subunit tests described above address virtually all of the principal performance issues except that of waveform design and range/velocity ambiguity resolution. Thus, the end-to-end tests focus on the issues which arise in such testing. First, however, it is necessary to very briefly review some of the key considerations which arise in choosing waveform design and the range/velocity unambiguity resolution logic.

Range/velocity ambiguity resolution is discussed in detail in Doviak and Zrnic' (1984). If the system designer chooses to use an equally spaced train of pulses (which is advantageous for clutter suppression and weather parameter estimation), the unambiguous range (R_a) and Nyquist velocity (V_n) are related by

$$R_a V_n = c\lambda/4$$

where λ = the wavelength, $R_a = cT/2$, $V_n = \lambda/2T$, and T = the interpulse spacing. Figure II-3 shows the tradeoff between R_a and unambiguous velocity ($V_u = V_n/2$) for S-band and C-band radars. The TDWR will provide reflectivity, velocity and spectrum width data to approximately 89 km. That yields an unambiguous velocity of approximately 22 m/s. Using of non-uniformly spaced pulse trains (e. g., blocks of pulses at a constant PRF or varying time spacing between each pulse) can effectively yield a larger value for R_aV_u at the expense of more complicated signal processing.

The effective range of velocity values can be extended by velocity unfolding algorithms which utilize spatial continuity arguments to detect and resolve velocity folds which occur when the actual velocity is greater than V_u. The TDWR specification requires such algorithms to achieve an effective unambiguous velocity interval of $\pm$ 40 m/s. The unambiguous range extent can also be increased by use of measurements with various pulse spacings.

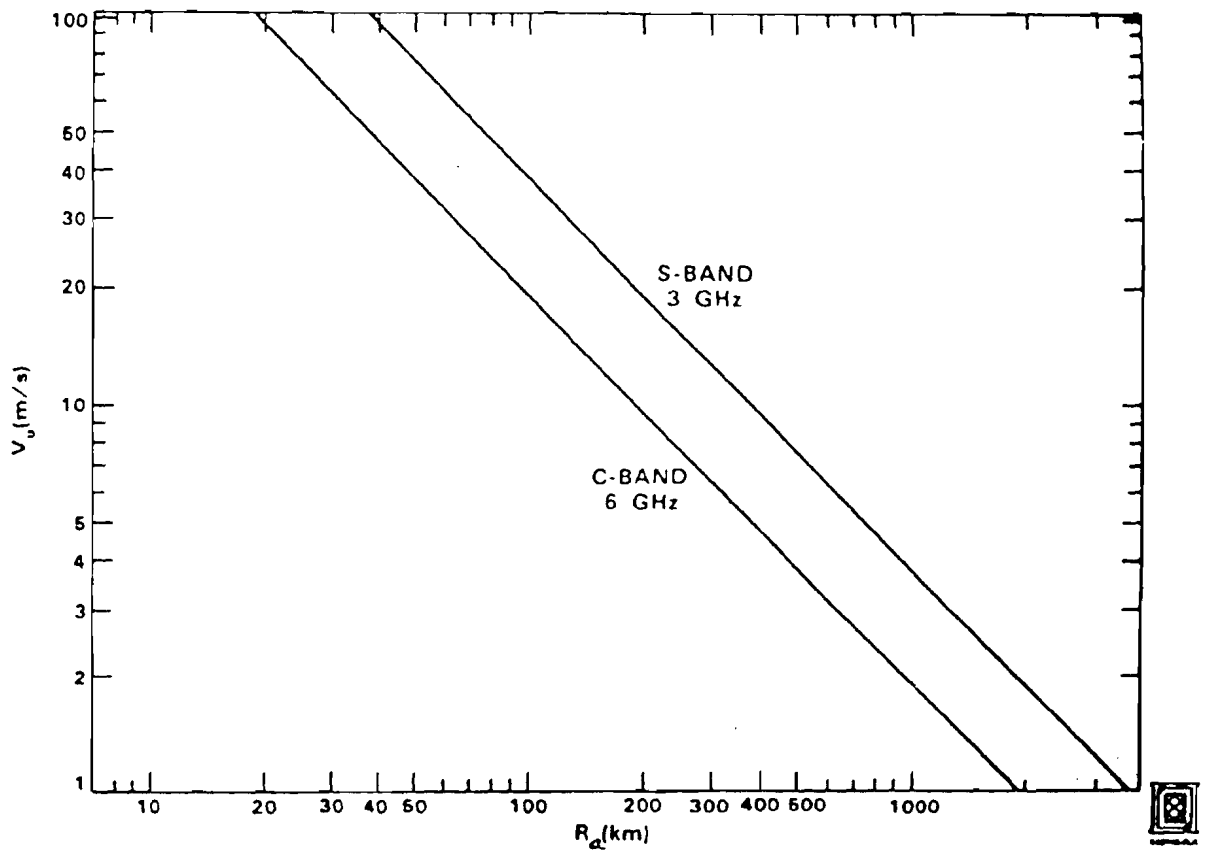

Figure II-3. Unambiguous doppler velocity (V_u) vs unambiguous range (R_a).

The two other design consideration in choice of signal waveform and range/velocity unfolding are (1) basic weather parameter accuracy (which depends primarily on the product $\sigma_w T$ with σ_w the weather spectral spread, the estimation algorithm, and the signal waveform used) and (2) avoiding obscuration by out-of-trip weather.

Obscuration by out-of-trip weather is discussed extensively in Crocker (1987). Obscuration avoidance requires that the TDWR use interpulse spacings which minimize the liklihood of out-of-trip weather (i. e., weather at ranges > R_a) being range aliased so as to obscure the weather return from critical regions (e. g., over the airport runways). The specification calls for the ability to vary the basic unambiguous range (i. e., cT/2 where T is the interpulse spacing) by 50 km. Thus, if a constant PRF signal waveform were used for the TDWR, with no special means being used to extend the measurement range, the unambiguous velocity would range from 22 m/s (at 90 km range) to 14 m/s (at 140 km range).

The discussion above shows that a constant PRF signal sequence cannot meet all the TDWR objectives for unambiguous range and velocity measurements simultaneously without some additional software features (e. g., a velocity dealiasing algorithm). The Nyquist velocities which correspond to the interpulse spacings may be such that there is some degradation of accuracy for large weather spectrum widths over that for an S-band system with the same pulse spacing due to loss of echo coherence (Doviak and Zrnic' 1984). Also, since differential velocities in microburst events have been observed which exceed 30 m/s, we see that some degree of velocity folding is likely to occur on at least an interpulse basis with the TDWR if the range obscuration avoidance objectives are to be achieved.

Since the actual set of interpulse spacings used by the TDWR contractor will interact with both the clutter processing and the weather parameter estimation, it is necessary to consider simulations at the time series level to insure that all of the processing factors are properly considered in arriving at the base product estimates and algorithm outputs. The quotation below from the technical specification describes the specific tests to be performed using the storm model data sets to be provided.

> 4.2.1.13 Signal Processing Simulation Test. The signal processor functions shall be tested, in the context of the complete system, by the injection of simulated and actual test data. This data shall be generated in accordance with the Government supplied weather event models and specfic data cases described in Engineering Report DOT/FAA/PM-87-37. Simulated signal processor inputs shall be generated from the idealized weather models and case data, to mimic the effects of range and velocity aliasing, SNR, and parameter estimation errors. This simulated data shall then be injected into the signal processor. All signal processor and RDA functions shall be invoked on the simulated input data, and the resulting base data sent to the RPG for algorithm processing. Verification of the signal processor functions shall be accomplished by comparison of the base data and the algorithm outputs to the weather models, and data corresponding to correct weather processing algorithms results. Each weather event model and specific data case shall be simulated at each of the PRF values the contractor plans to use for wind shear detection.

Base data accuracy as determined by this test shall meet or exceed the accuracy requirements of this specification.
Microburst and gust front detections on the simulated data must match the Government supplied correct algorithm outputs with a detection probability of at least 0.98 and a probability of an alarm being false of 0.02.

NOTE: This test is designed to verify that the data quality functions in the signal processor are adequate to support the weather processing algorithms in the RPG. Test cases and weather event models are chosen to stress the signal processor, and adequate performance (compared to the algorithm operating on the ideal data) on this small set of test cases will provide confidence that the specific system implementation fully supports the meteorological processing algorithms. The choice of PRF is determined by the spatial distribution of weather at long ranges. Since the TDWR should detect microbursts over the airport for any PRF that was necessitated by the out of trip weather, performance must be verified at all of the possible PRF values.

(The quotation above is for convenience of the reader. When implementing this document, the latest revision of Paragraph 4.2.1.13 of FAA-E-2806 should be used.)

In view of the likelihood of velocity folding on an interpulse basis with a C-band TDWR, the initial set of cases used for the end-to-end testing have focused on strong velocity events. These are also important events operationally. However, as discussed in Chapter IV, it will also be necessary to consider additional cases which may be stressful for velocity unfolding due to missing data (e. g., from low SNR and/or high residual clutter levels).

The models to be provided will consist of base product data sets in polar format (range, azimuth and elevation) on approximately the same spatial grid as the TDWR base products (1 degree in azimuth, 150 m in range) and with a representative hazardous weather scanning mode.

III. CHARACTERISTICS OF WEATHER MODELS FOR END-TO-END TESTING

A. C-BAND TDWR VS. S-BAND TDWR TEST-BED RADAR DATA

The actual data sets derived from an initial pair of weather models will be furnished on Universal weather radar format digital tapes to facilitate computer generation of the simulated time series waveforms. As explained above, the FAA TDWR S-band test-bed radar (Evans and Johnson, 1984) has been used to obtain data sets so that there will be a minimum of contamination by ground clutter. The measured velocities provided on the data tapes will have been corrected for velocity folding by a combination of automatic unfolding (using radial continuity) and manual correction. The spectrum width and reflectivity estimates will not have been modified nor will any smoothing have been applied to the velocity data so that the various contributions by the "natural" sources will be present in the data sets.

The applicability of the S-band data sets to the C-band TDWR is an issue which warrants some discussion. The sensitivity of the TDWR S-band test-bed is similar to that of the C-band TDWR, so that the data should be representative in terms of signal-to-noise ratio (SNR). C-band TDWR sensitivity is such that low SNR is likely to be an issue when the clear air return is the principal source of scattering. If the return were from refractive index inhomogenities, S-band would have a higher effective reflectivity in terms of dBz than would C-band. However, it appears that during the summer seasons when the bulk of microbursts appear, that the principal scattering is from insects and dust particles; in which case, the reflectivities measured in dBz would be identical for the two frequencies. The data sets provided then, should <u>not</u> be degraded to create a lower SNR at C-band.

The C-band TDWR will use an 0.5 degree beamwidth with azimuth coherent processing intervals (CPI) of 1 degree while the S-band TDWR testbed has a 1 degree beamwidth with, nominally, a 1 degree CPI. (There is a small difference in the effective azimuth extent of the two systems, but it should be negligible given the azimuth extent of the phenomena of concern.) Although the altitude extent of the resolution volumes differ by a factor of 2, that should not materially affect the nature of the data fields. The features of concern are, typically, much thicker than the resolution volume vertical extent.

As discussed above, the S-band data sets will have considerably less velocity folding for the unambiguous range used than would be the case had C-band been used for the initial measurements. However, that is a virtue in the present application since considerable effort has been expended in removing velocity folds from the data sets to be provided.

The major potential difference is in the degree of clutter contamination of the velocity fields. It appears that the actual reflectivity of typical windshear fields is higher at C-band (due to the Rayleigh scattering) while the ground clutter at C-band is not corresponding higher. In addition to the basic scattering difference, the narrower elevation beam of the C-band TDWR will enable it to avoid illuminating clutter sources with the mainbeam in situations where the S-band TDWR test-bed would encounter mainlobe clutter. There is no means for correcting for those differences in the data sets provided. However, in both cases the areas in which windshear occurs are not regions in which the S-band TDWR test-bed encountered high levels of clutter.

Additionally, it could be argued that the data sets simply correspond to a more stringent but still "representative" clutter environment at C-band than did data sets taken at the actual site.

Depending on the waveforms used by the TDWR contractor, there may be situations within these data sets where a C-band system would have a higher variance in the velocity and spectrum width base products due to a higher degree of data decorrelation. However, that will occur "naturally" as a byproduct of the time series simulation process and need not occur explicitly as a modification to the provided data sets.

Thus, we conclude that the furnished data sets (albeit measured at a different frequency with a wider beamwidth) can be directly used as the input for the end-to-end simulation testing without any modification of the provided base product data.

B. MOIST SUBCLOUD ENVIRONMENT STORM MODEL A

Measurements in the Memphis, TN, and Huntsville, AL, areas during 1984-86 have shown that wind shear events occur fairly frequently in the humid environment characteristic of the southeast portion of the United States [Rinehart, DiStefano, Wolfson (1987), Wolfson, DiStefano, Fujita (1985), Rinehart, Isaminger (1986), Wolfson (1988)]. Microbursts in this area are characterized by significant amounts of rain (e. g. reflectivities in the core region of greater than 40 dbz) associated with the downdraft region.

The Huntsville, AL, observations had a faster scan rate than was available in Memphis and hence were viewed as better from the viewpoint of storm model generation. On 21 September 1986, weak boundary layer winds, surface heating, and an ample moisture supply provided for scattered air-mass activity. The cells were primarily stationary. Sixteen microbursts and one gust front were detected in a $2\frac{1}{2}$ hour period. That represents a record for daily microburst detections for both Memphis and Huntsville.

One of the strongest shears was the Decatur Downburst at 20 km range, 250° azimuth at 1929 GMT (Fig. III-1)*. A velocity couplet of +27 and -9 m/s occurred over a distance of 2.7 km. There was extensive damage in the Decatur area from that outflow. The winds snapped power poles, trees, and overturned a tractor-trailer rig. Another strong divergent signature was detected 20 to 30 minutes later at range 21 km, 208° azimuth (Fig. III-2). The differential velocity was 39 m/s over 4.0 km.

C. DRY SUBCLOUD ENVIRONMENT STORM MODEL A

Measurements in the dry subcloud environment near Denver (Fujita, 1985, Hjelmfelt, 1988, Wolfson, 1988) have shown a high frequency of wind shear occurrence (especially, microbursts). Due to evaporation of precipitation below the cloud base, microbursts can occur in the high plains

*Expanded plots of the reflectivity, radial velocity and spectrum width fields shown in Figures III-1 to III-4 are provided in Appendices A-D.

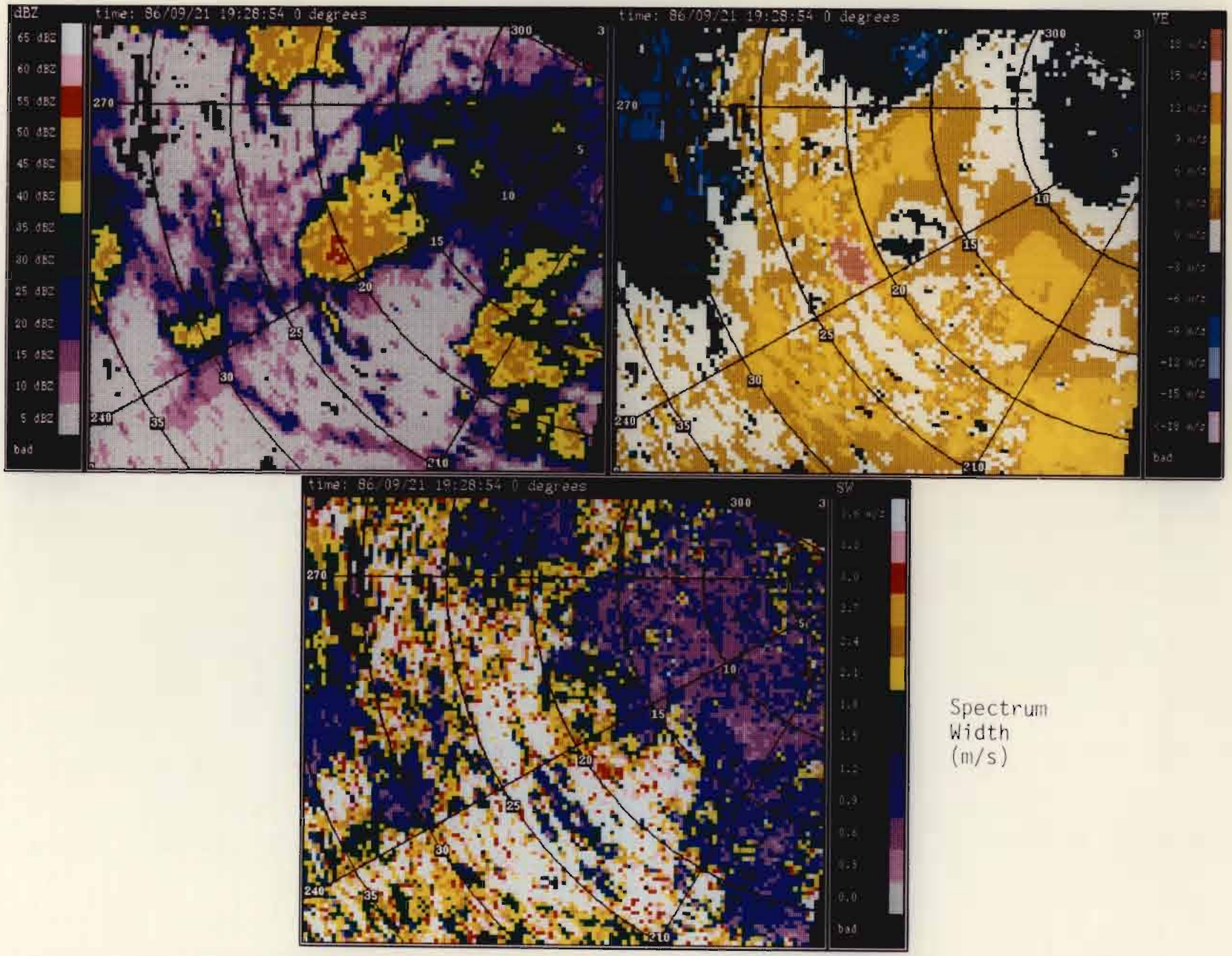

Reflectivity (dBZ)

Radial Velocity (m/s)

Spectrum Width (m/s)

Figure III-1. Characteristics of Decatur, AL, microburst at 1929 GMT on 21 September 1986.

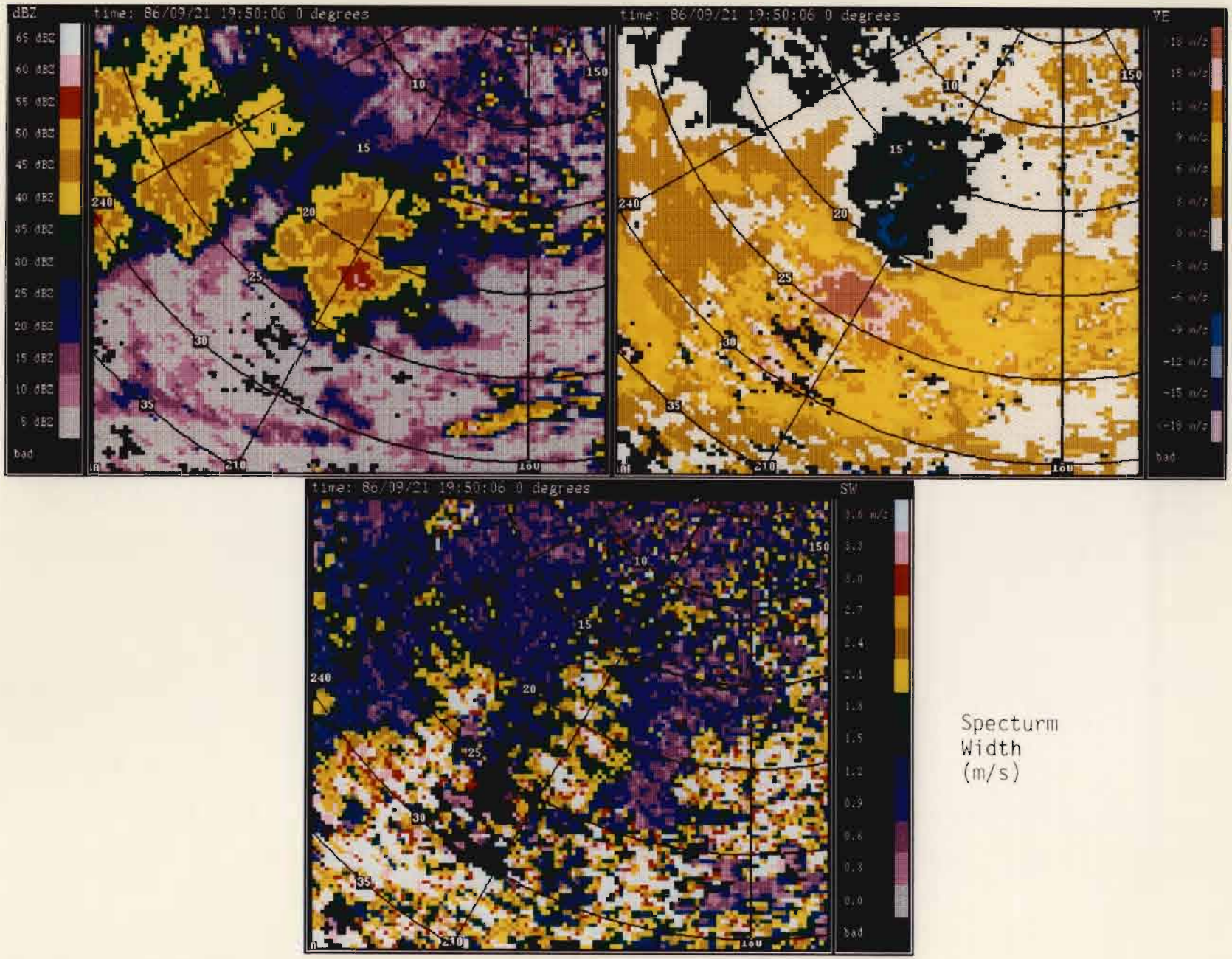

Reflectivity (dBZ)

Radial Velocity (m/s)

Specturm Width (m/s)

Figure III-2. Characteristics of Decatur, AL, microburst at 1951 GMT on 21 September 1986.

area with so little rain reaching the ground that the ground is not wetted (i. e., a "dry" microburst) and low radar reflectivites occur in the core and outflow regions. Microbursts of the type observed in the southeast portion of the U. S. do occur, but are less common in Denver than in Huntsville or Memphis.

On 15 June 1987, the FAA test-bed TDWR observed a mixture of low and moderate reflectivity microbursts. Figures III-3 and III-4 show the surface base product data at two representative times. At 1443 local time a strong microburst is located WSW of the radar with peak differential velocities of approximately 28 m/s. That particular case is challenging at this time for velocity unfolding due to the missing data between the microburst and the radar due to low reflectivity of the clear air return. Some 43 minutes later, the storm system had moved eastward and split to create several moderately strong microbursts southwest and south of the radar with differential velocities of approximately 15-20 m/s.

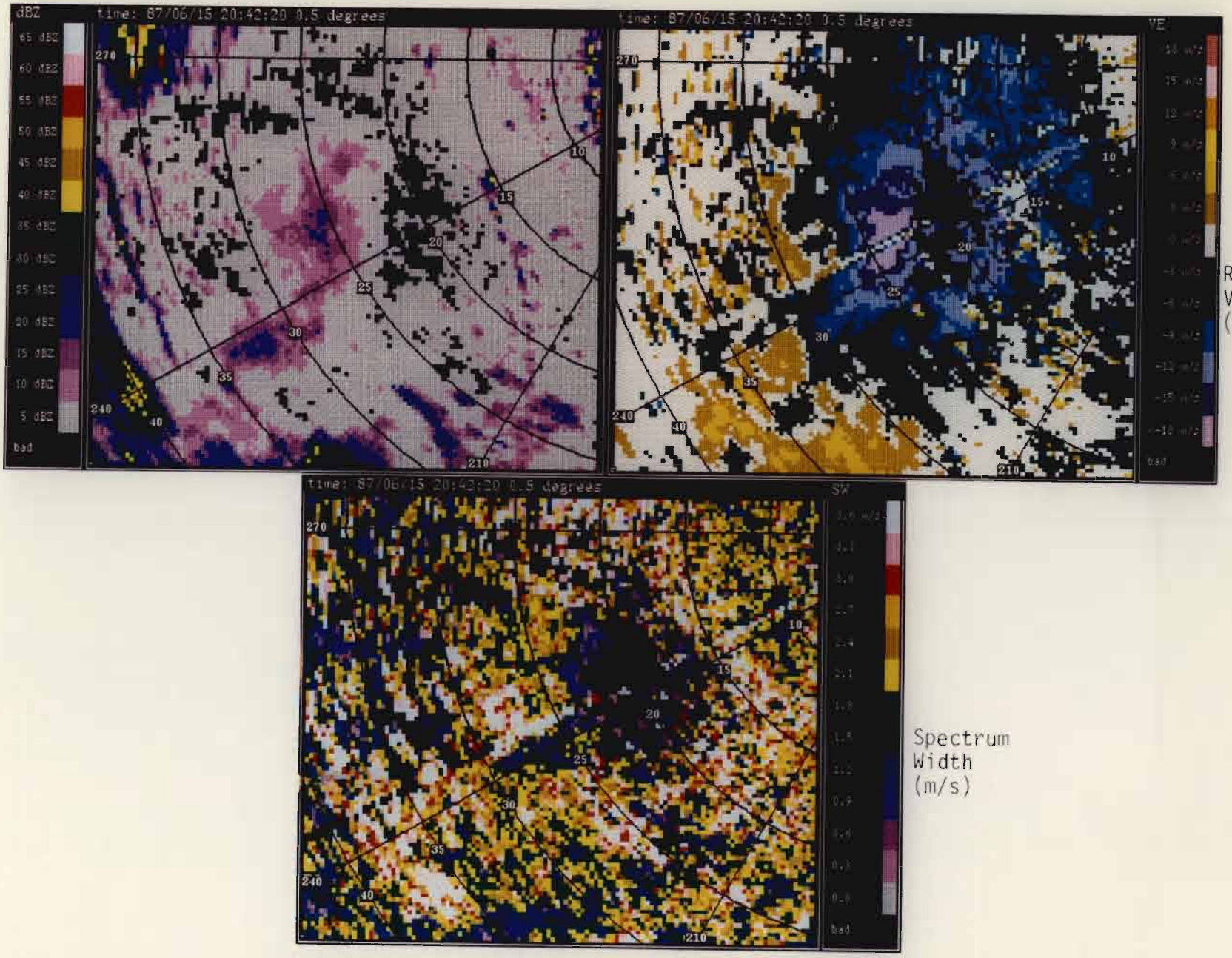

Figure III-3. Characteristics of Denver, CO, microburst at 2042 GMT on 15 June 1987.

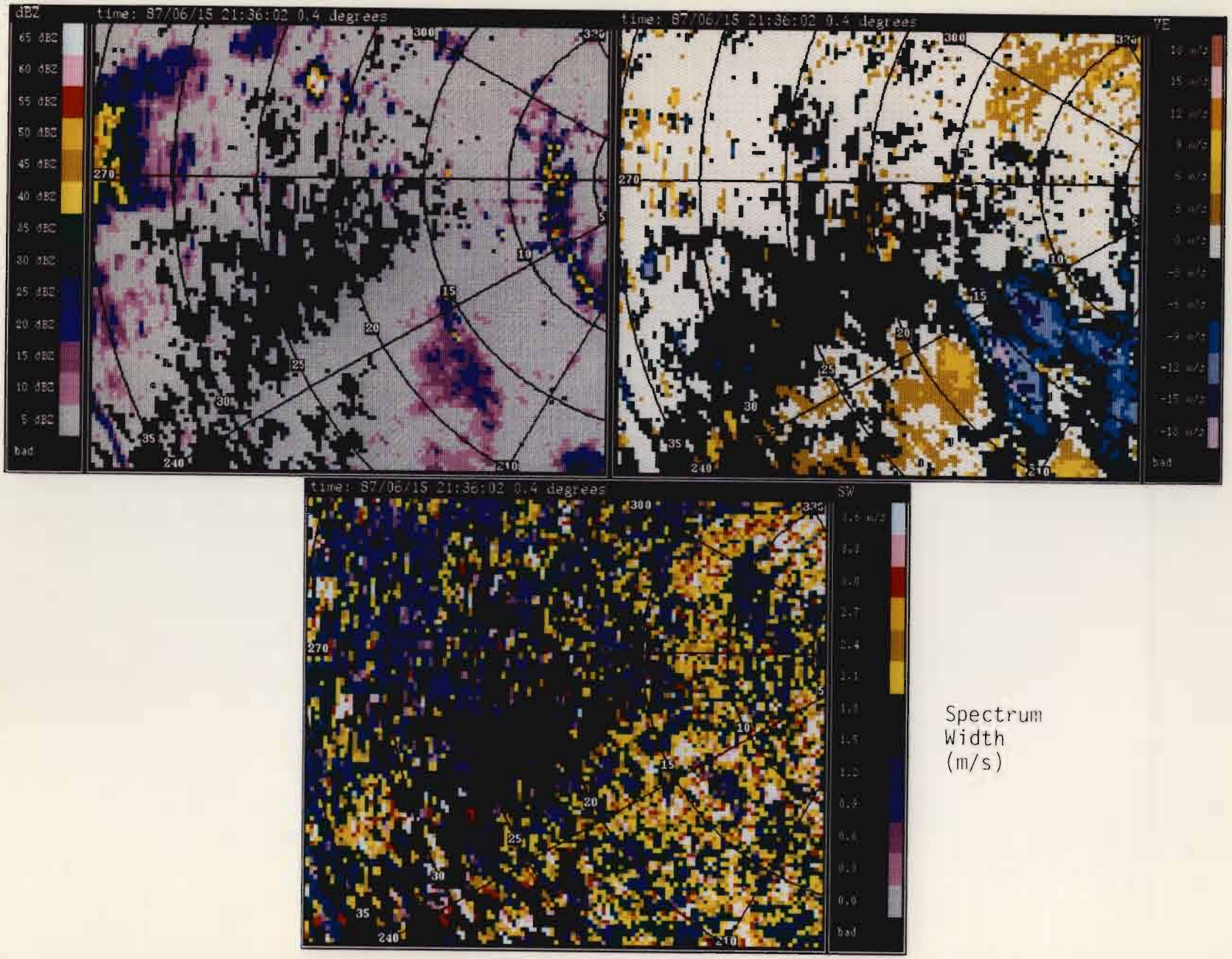

Figure III-4. Characteristics of Denver, CO, microburst at 2136 GMT on 15 June 1987.

IV. SUMMARY AND CONCLUSIONS

In this report, we have discussed the principal considerations in qualifying the TDWR contractor design from the viewpoint of performance in detecting hazardous windshear (especially microbursts) as a backdrop to the discussion of the initial weather models for end-to-end testing. We saw that although the bulk of the key RDA and RPG system features are validated both on a subsystem basis and by individual system testing, there are some performance factors associated with the choice of signal waveform and range/velocity aliasing which are contractor dependent that could effect system performance.

The practical difficulty in arranging for standard "storms" with appropriate supporting weather measurement systems at the test site used for the first system Qualification Test and Evaluation has led to the use of end-to-end simulation testing using government furnished storm models (based on measured and model storms) to validate the contractor approach to signal waveform and range/velocity aliasing. By reviewing the pertinant aspects of signal waveform choice, we conclude that the velocity dealiasing will be the factor of principal concern in this area and that weather models which stress velocity dealiasing should be emphasized in the end-to-end testing.

The cases from Huntsville, AL, and Denver, CO., discussed in Chapter III represent some of the strongest microburst events (in terms of velocities) observed by the FAA TDWR radar in some three years of windshear testing. Those cases will provide a challenging test of velocity unfolding to support microburst detection.

However, additional cases may be required to address other, less critical elements of wind shear detection, including

(1) cases which stress the ability to estimate the winds behind a gust front for purposes of estimating the wind shift associated with gust front passage. (Since the algorithm currently used to estimate wind shift requires velocities which are accurate in an absolute sense [as opposed, e. g., to radially continuous velocities], that particular application may be more stressful [albeit less critical operationally] than microburst detection insofar as velocity folding is concerned);

(2) cases where there is an substantial loss of data within a critical portion of the wind field (e. g., due to very high clutter as a gust front passes over a major city); and

(3) additional cases from the Denver and Huntsville TDWR test-bed measurement programs as further detailed analysis of these datasets continue.

As these additional cases are developed, this report will be updated to reflect all test data sets.

ACKNOWLEDGMENTS

The storm cases discussed in Chapter III were identified by Mark Isaminger based on his analysis of the TDWR test-bed measurements over the past three years. Additional assessment of the representativeness of the datasets was accomplished by Marilyn Wolfson. Michael Donovan accomplished the velocity unfolding using a combination of automated radial continuity unfolding with hand correction of incorrectly unfolded regions. Robert Hallowell carried out microburst detection algorithm runs on the datasets to further refine the shear levels.

REFERENCES

Crocker, S.C., 1987: "TDWR PRF Selection Criteria", Project Report ATC-147, Lincoln Laboratory, MIT, DOT/FAA/PM-87-25 (in press)

Doviak, R.J., and D.S. Zrnic', 1984: Doppler Radar and Weather Observations, Academic Press, New York

Evans, J.E. and D. Johnson, 1984: "The FAA Transportable Doppler Weather Radar", Preprints, Twenty Second Conference on Radar Meteorology, pp. 246-250, American Meteorological Society, Boston, MA.

Federal Aviation Administration, 1987: Terminal Doppler Weather Radar Specification, FAA-E-2806 (6 Oct. 1987)

Fujita, T.T., 1985: The Downburst, Microburst and Macroburst. University of Chicago, 122 pp.

Hjelmfelt, M.R., 1988: "Structure and Life Cycle of "Microburst Outflows Observed in Colorado", Jour. of Climate and Applied Meteor. (in review)

Merritt, M. and S. Campbell, 1987: "Microburst Detection Algorithm" Project Report ATC-145, Lincoln Laboratory, MIT, DOT/FAA/PM-87-23 (in press)

Rinehart, R.E., and M.A. Isaminger, 1986: "Radar Characteristics of Microbursts in the mid south", 23rd. Conference on Radar Met., Snowmass, pp. J116-119

Rinehart, R.E., J.T. DiStefano, and M.M., Wolfson, 1987: "Preliminary Memphis FAA/Lincoln Laboratory Operational Weather Studies", Project Report ATC-141, Lincoln Laboratory MIT DOT/FAA/PM-86-40 (22 April 1987)

Sanford, P., A. Witt and S. Smith, 1987: "Gust Front/Wind Shift Detection Algorithm", Project Report ATC-146, Lincoln Laboratory, MIT DOT/FAA/PM-87-24 (in press)

Sirmans, D., D. Zrnic' and W. Bumgarner, 1976: "Estimation of maximum unambiguous Doppler velocity by use of two sampling rates", 17th Conf. on Radar Meteorol., 17th, pp. 23-28

Sirmans, D. and W. Bumgarner, 1975: "Numerical comparison of five mean frequency estimators", J. Appl, Meteorol. Vol. 14, 991-1003.

Wolfson, M.M., J.T. DiStefano, and T.T. Fujita, 1985: "Low-altitude wind shear characteristics in the Memphis, TN area based on mesonet and LLWAS data", Preprints, 14th Conference on Severe Local Storms, Indianapolis, Amer. Meteor. Soc., 322-327.

Wolfson, M.M., 1988: "Characteristics of microbursts observed in the continental US", Preprints, 15th Conference on Severe Local Storms, Baltimore, Amer. Meteor. Soc.

Zrnic', D.S., and P. Mahapatra, 1985: "Two Methods of Ambiguity Resolution in Pulse Doppler Weather Radar", IEEE Transactions on Aerospace and Electronic Systems, Vol. AES-21, No. 4, July 1985.

APPENDIX A

Figures A-1 through A-3 show the surface reflectivity, Doppler velocity and spectrum width features respectively of the Decatur, AL, microburst at 1929 GMT on 21 September 1986.

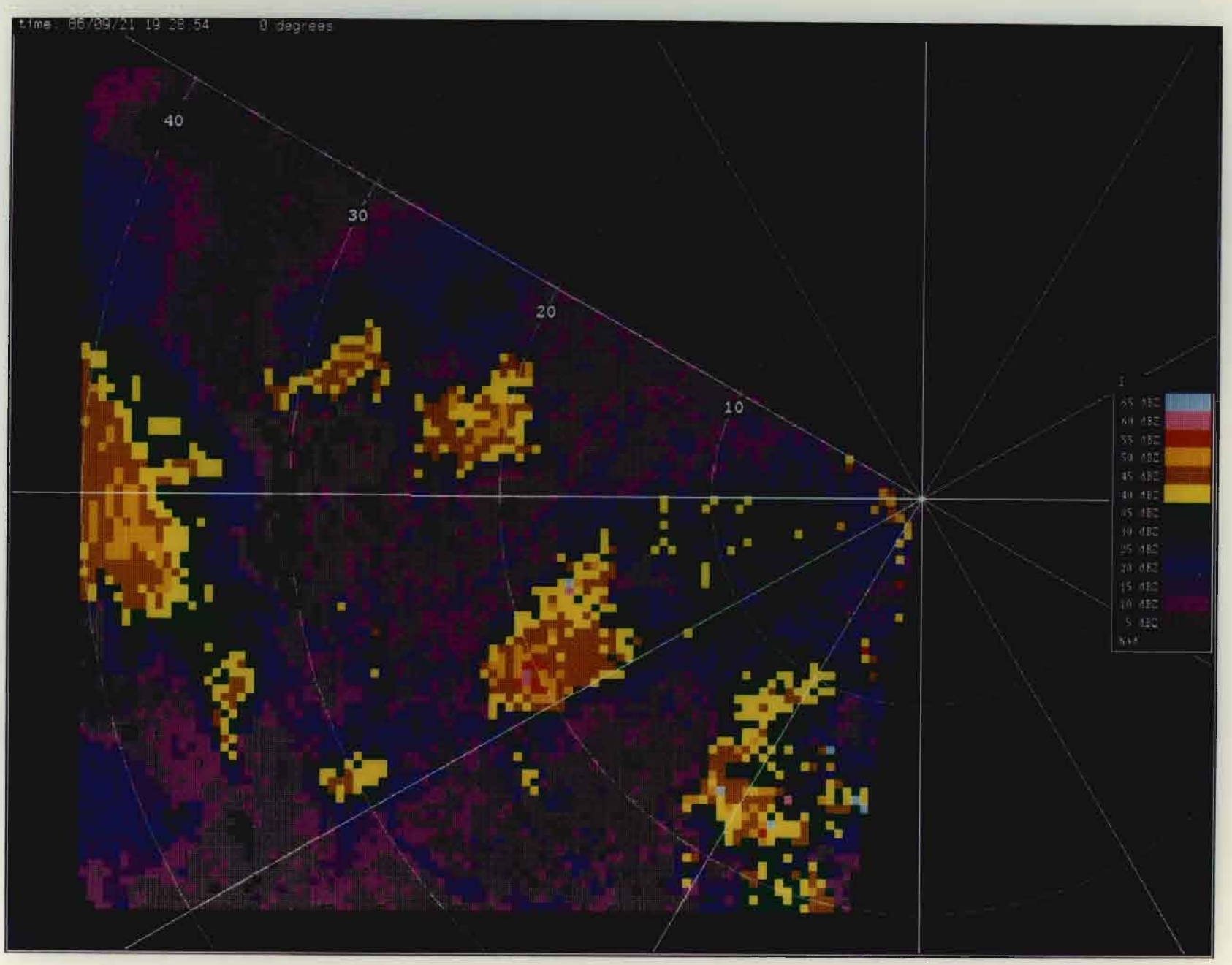

Figure A-1. Surface Reflectivity Field of Decatur, AL, microburst at 1929 GMT.

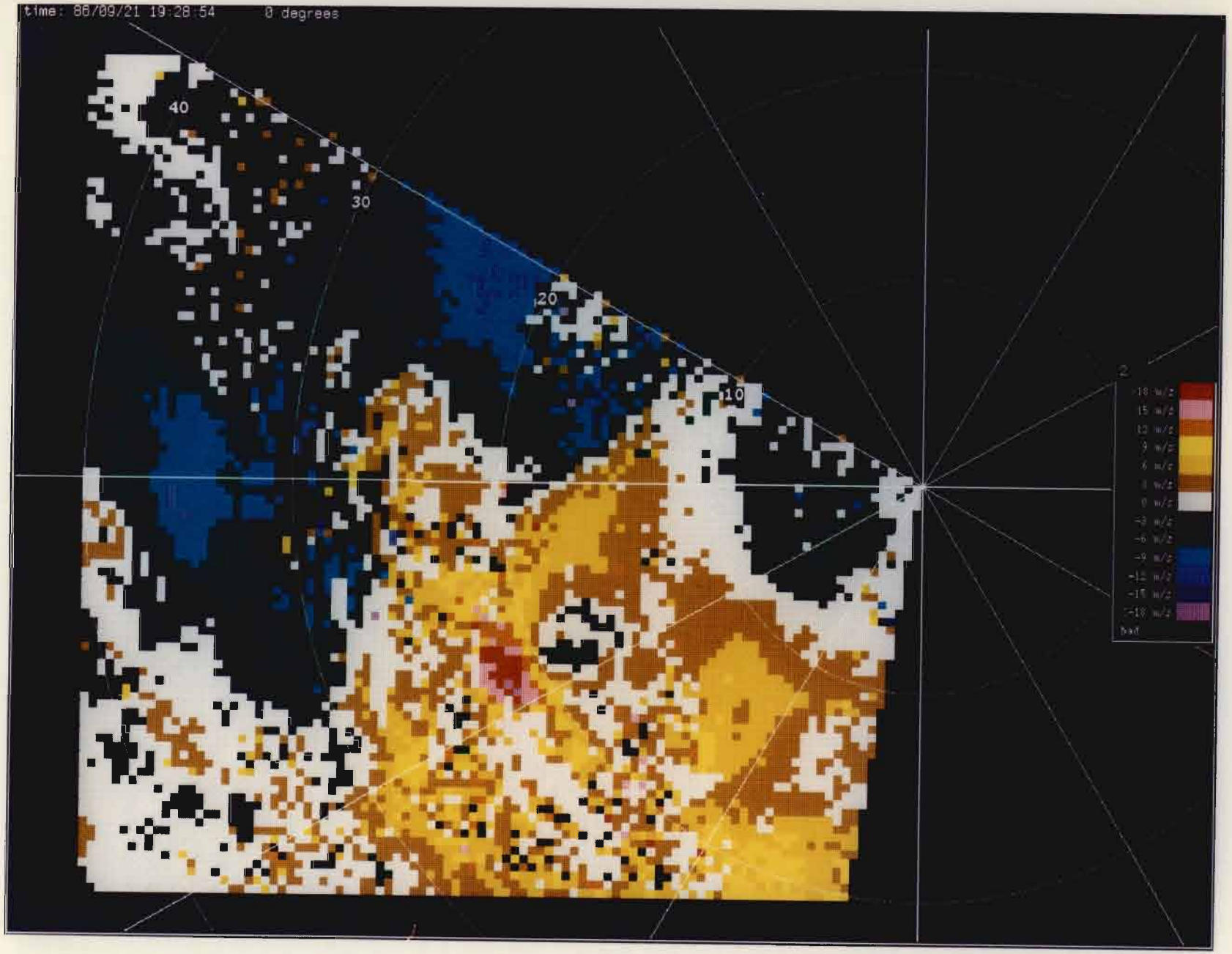

Figure A-2. Surface Velocity Field of Decatur, AL, microburst at 1929 GMT.

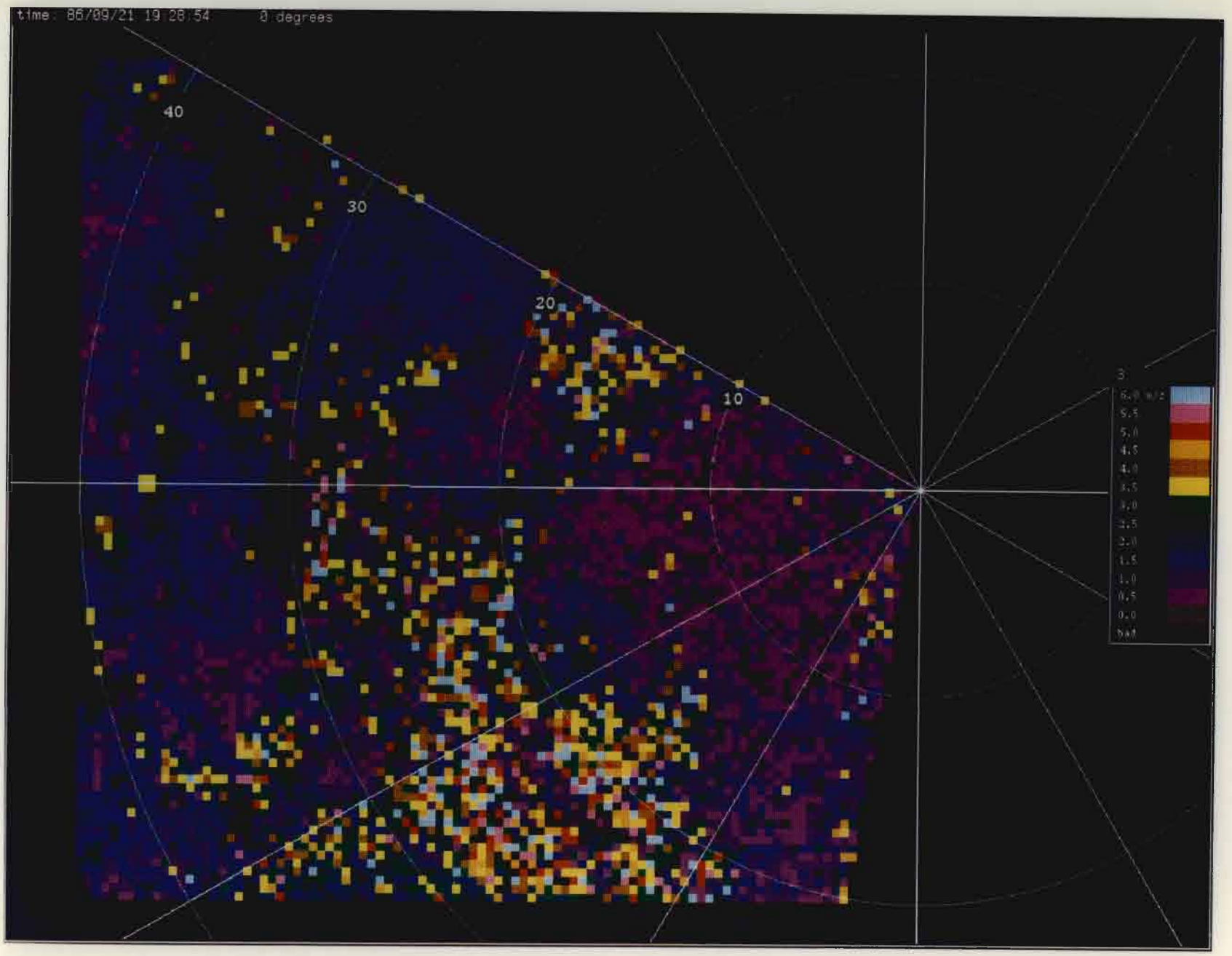

Figure A-3. Surface Spectrum Width Field of Decatur, AL, microburst at 1929 GMT.

APPENDIX B

Figures B-1 through B-3 show the surface reflectivity, Doppler velocity and spectrum width features of the Decatur, AL, microburst at 1951 GMT on 21 September 1986.

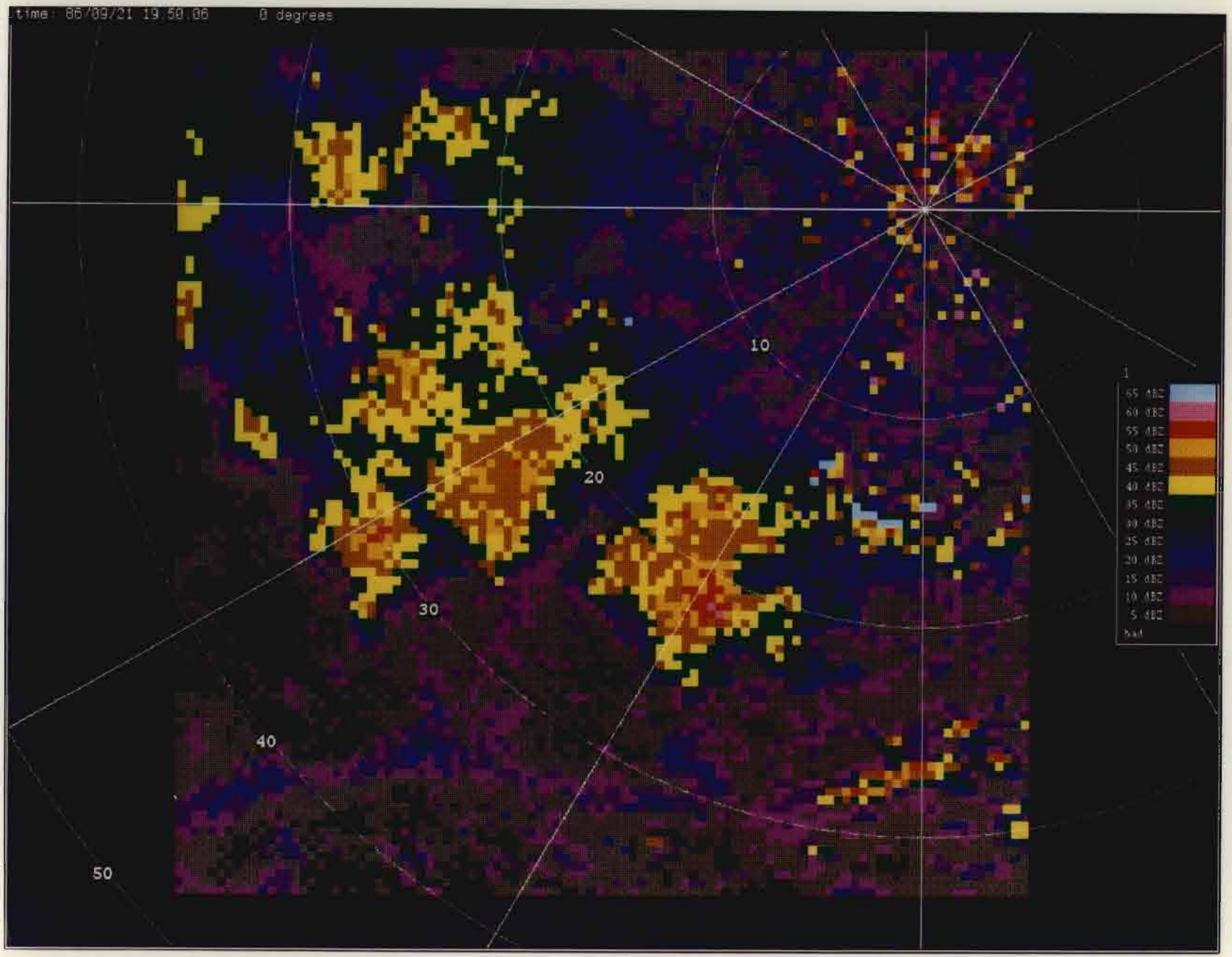

Figure B-1. Surface Reflectivity Field of Decatur, AL, microburst at 1950 GMT.

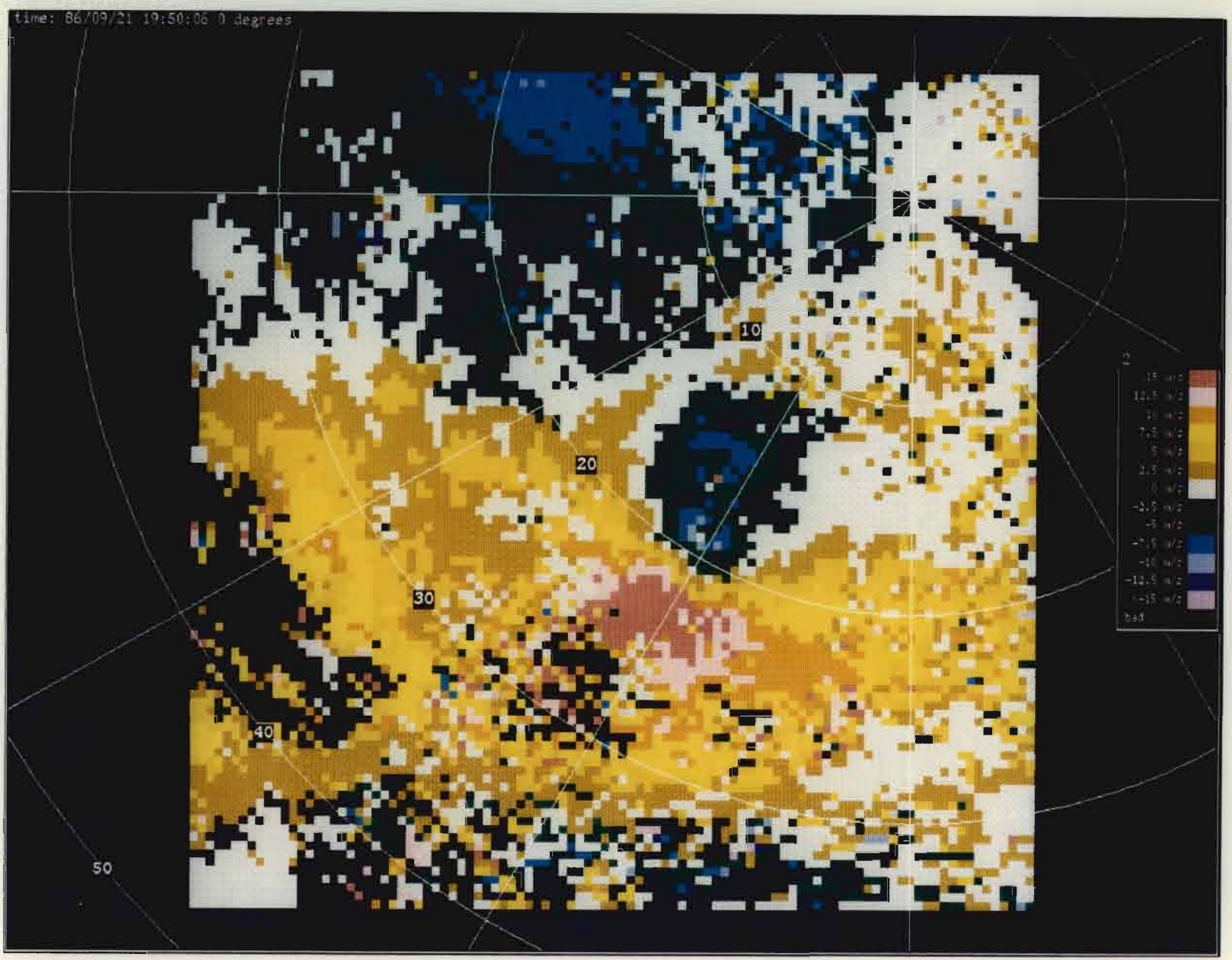

Figure B-2. Surface Velocity Field of Decatur, AL, microburst at 1950 GMT.

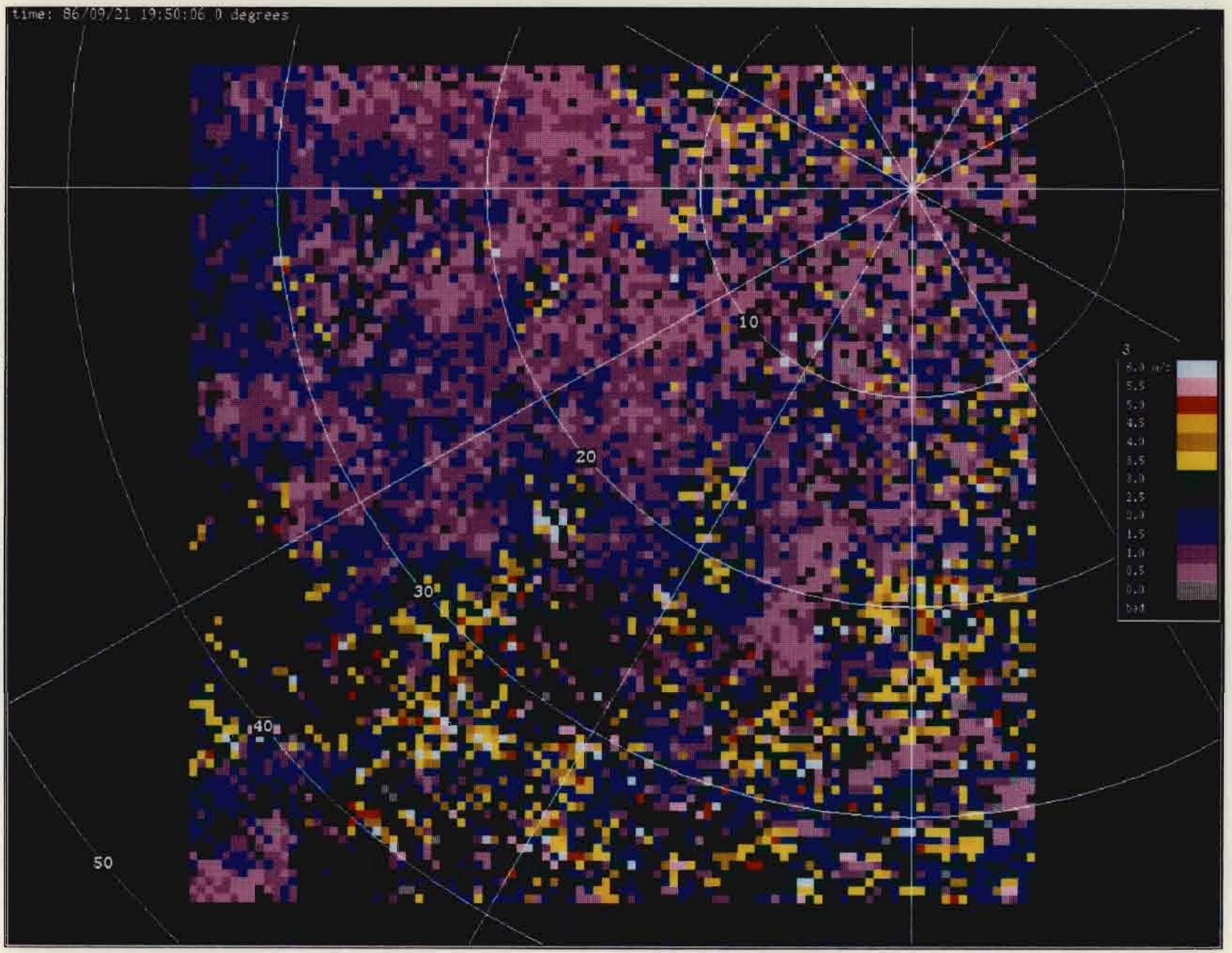

Figure B-3. Surface Spectrum Width Field of Decatur, AL, microburst at 1950 GMT.

APPENDIX C

Figures C-1 through C-3 show the surface reflectivity, Doppler velocity and spectrum width features of the Denver, CO, microburst at 1442 MDT on 15 June 1987.

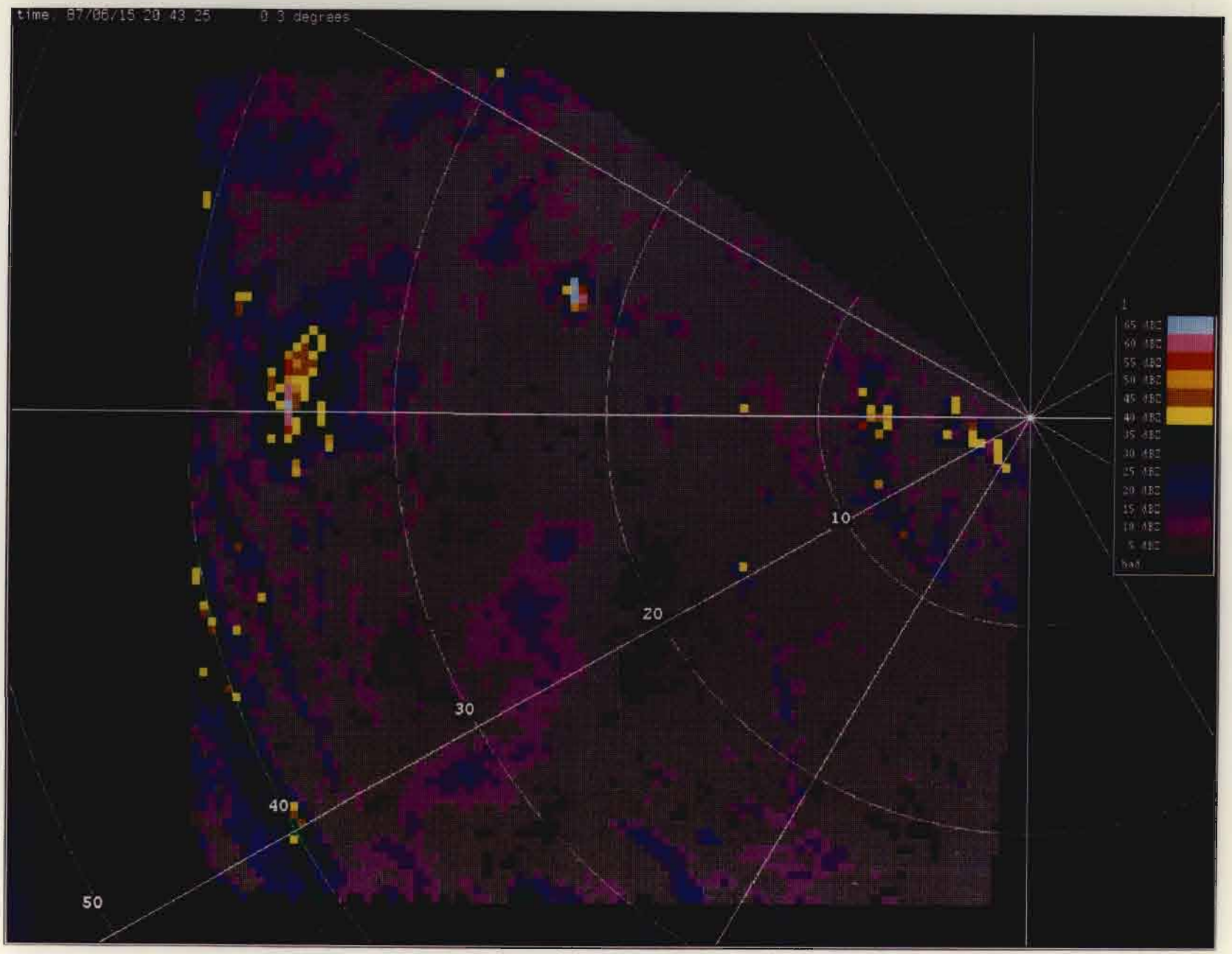

Figure C-1. Surface Reflectivity Field of Denver, CO, microburst at 2043 GMT.

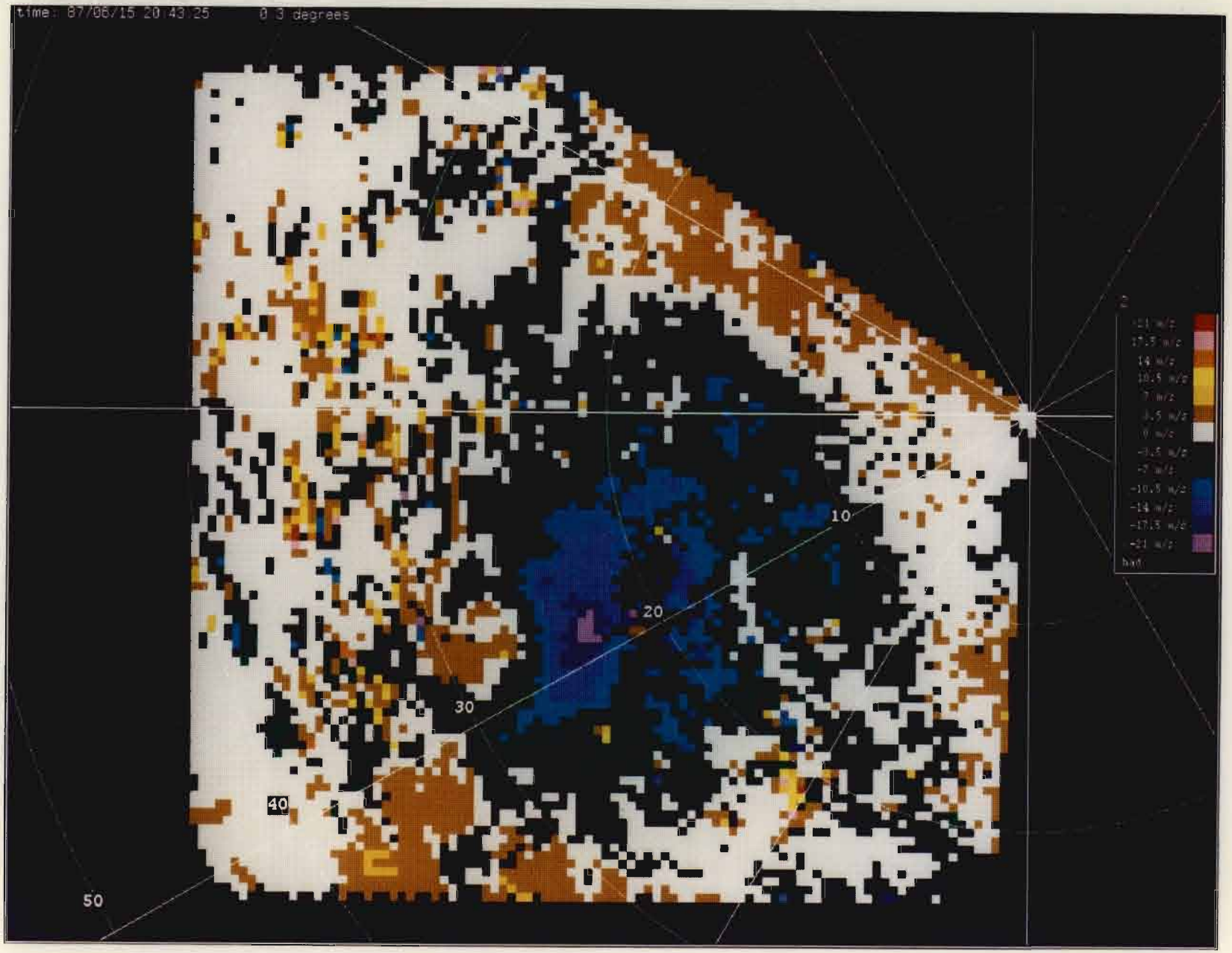

Figure C-2. Surface Velocity Field of Denver, CO, microburst at 2043 GMT.

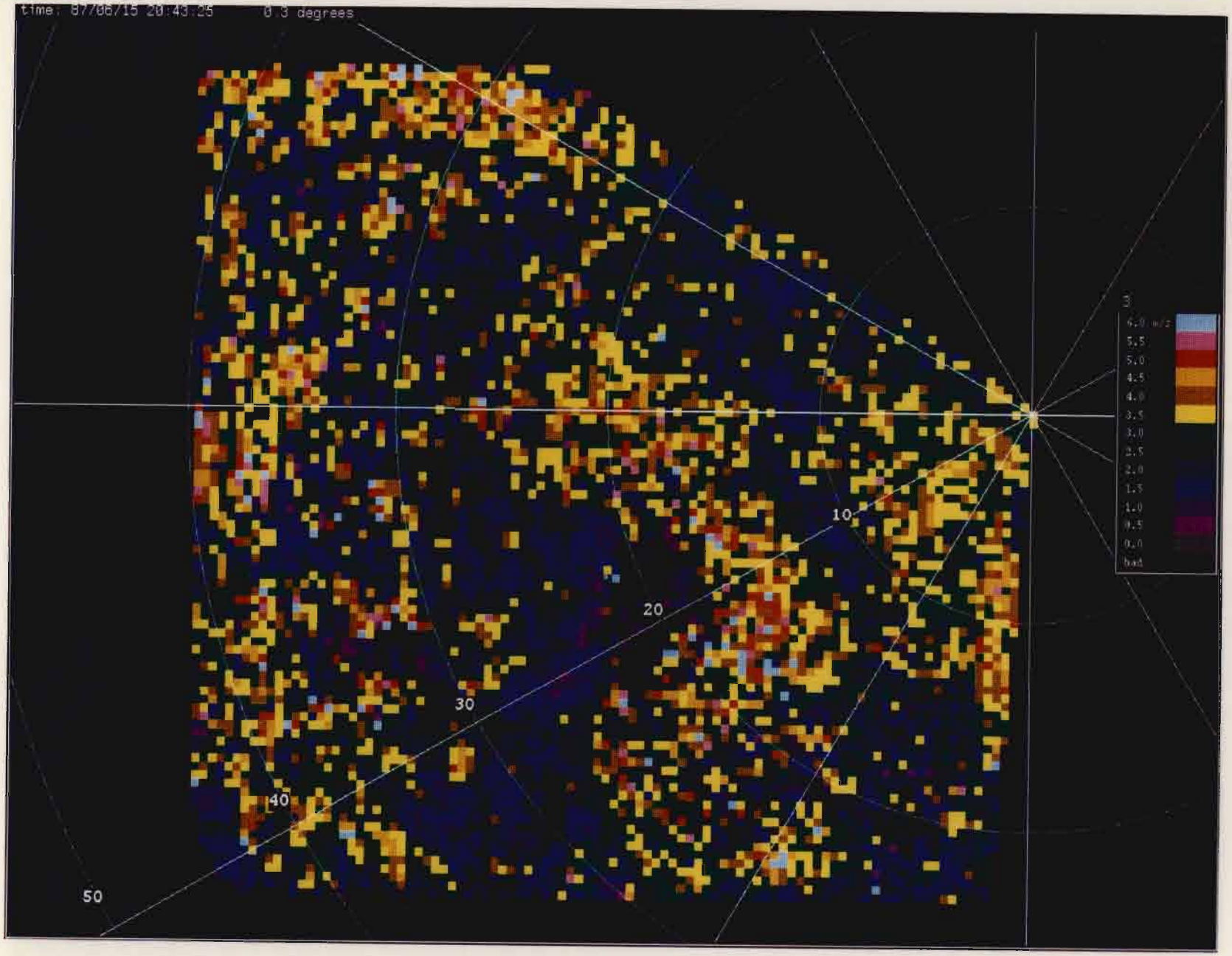

Figure C-3. Surface Spectrum Width Field of Denver, CO, microburst at 2043 GMT.

APPENDIX D

Figures D-1 through D-3 show the surface reflectivity, Doppler velocity and spectrum width features respectively of the Denver, CO, microburst occurring at 1536 MDT on 15 June 1987.

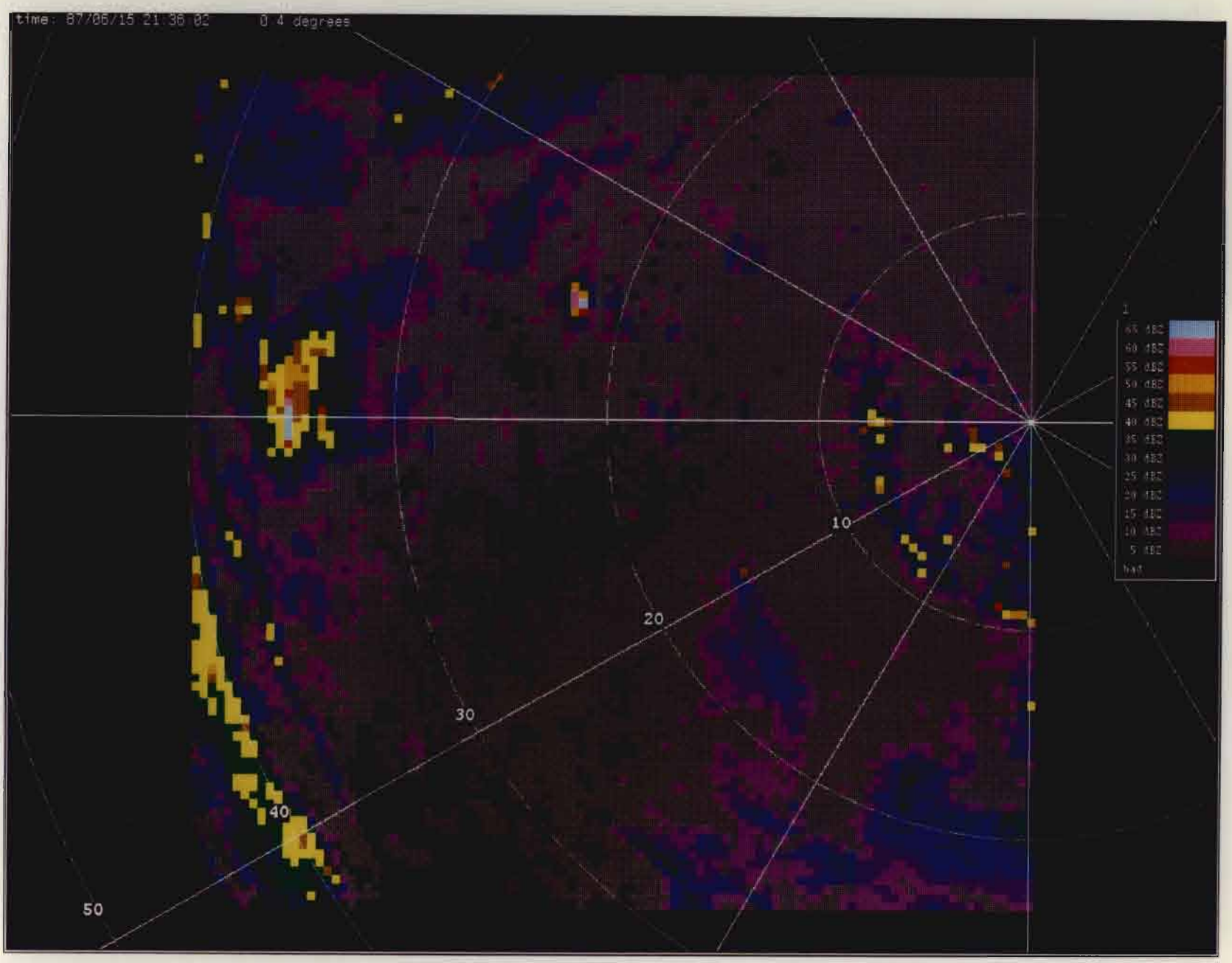

Figure D-1. Surface Reflectivity Field of Denver, CO, microburst at 2136 GMT.

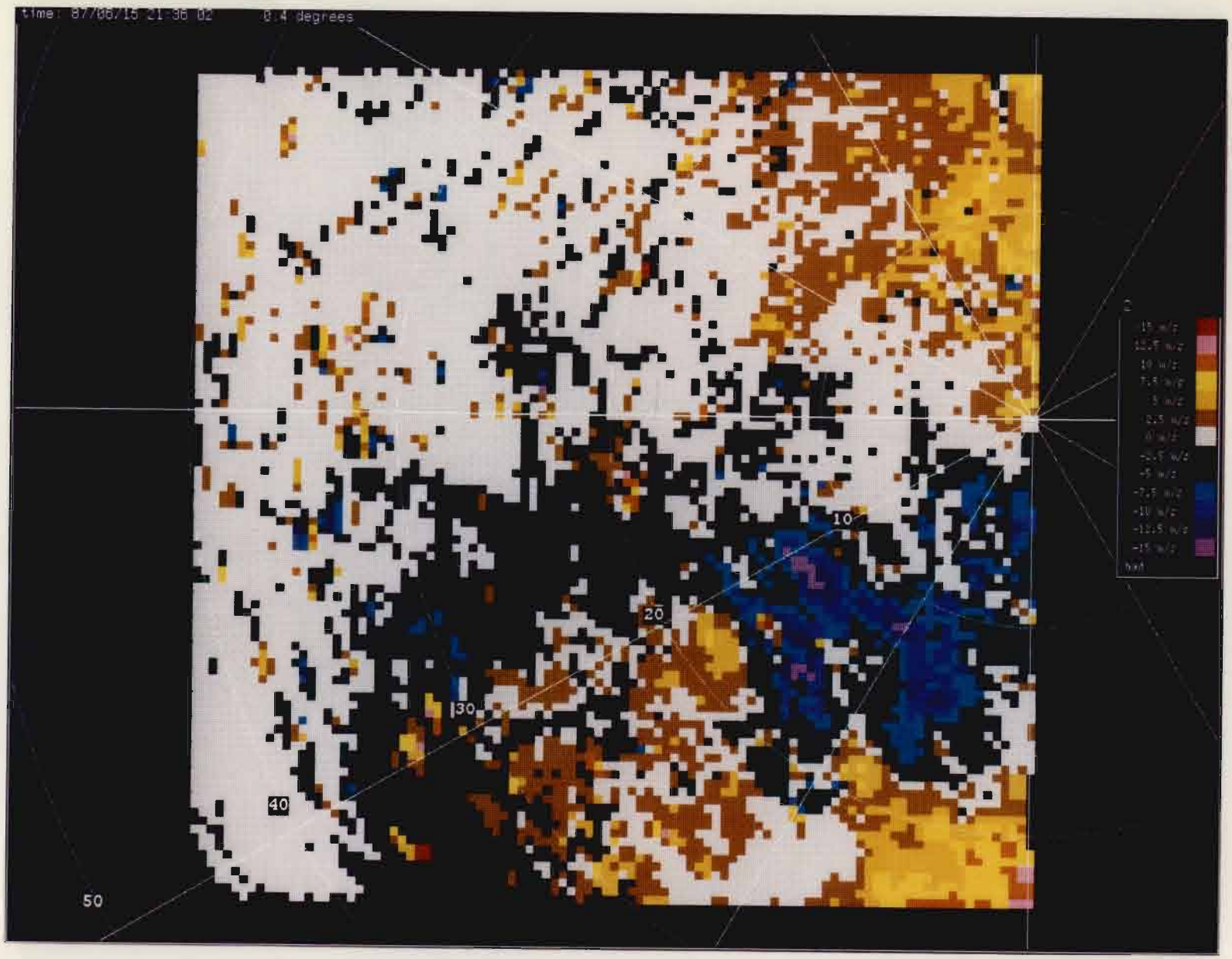

Figure D-2. Surface Velocity Field of Denver, CO, microburst at 2136 GMT.

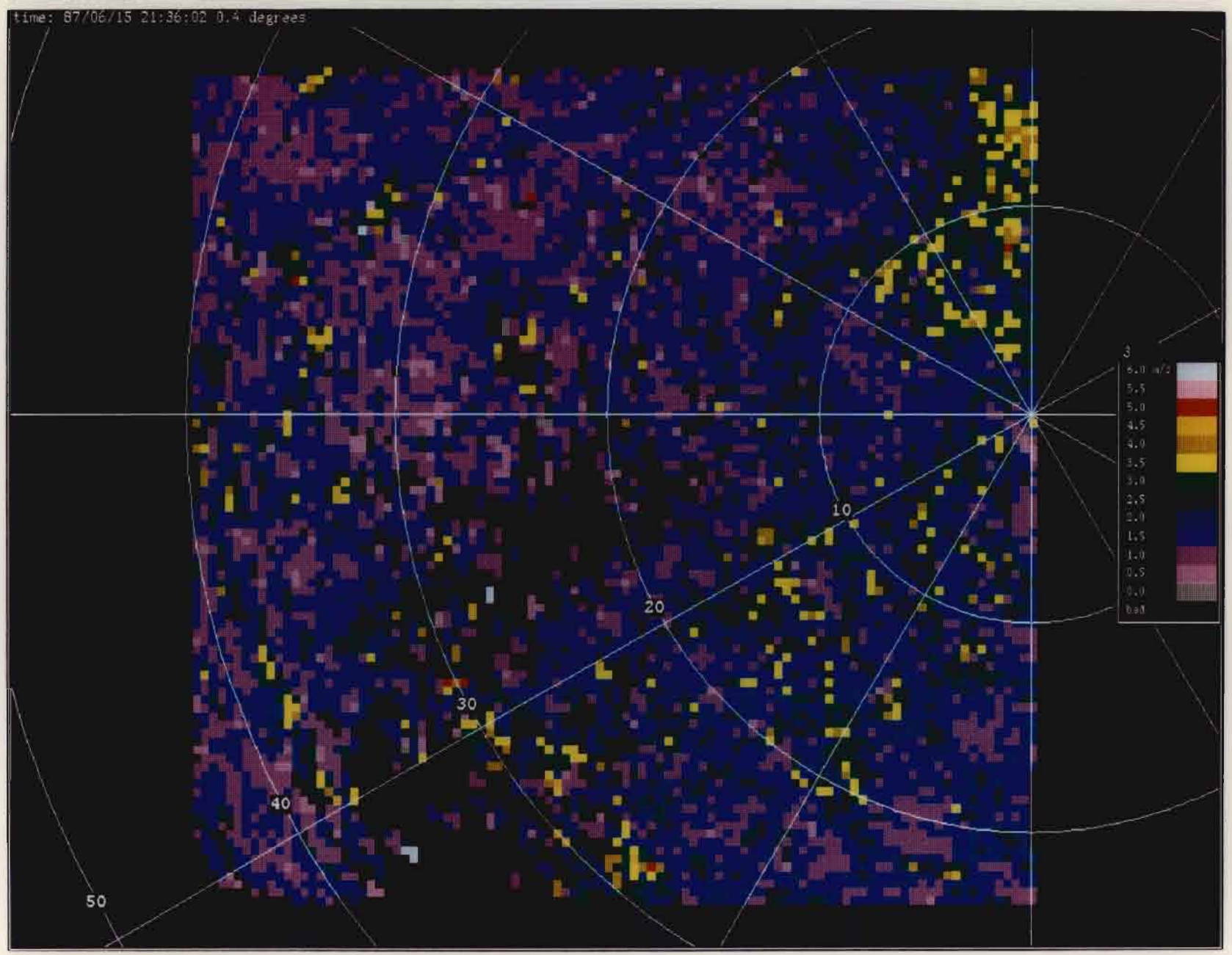

Figure D-3. Surface Spectrum Width Field of Denver, CO, microburst at 2136 GMT.